Water Quality Applications Of Satellite Remote Sensing

July 24, 1995

Proceedings

Water Quality Applications Of Satellite Remote Sensing

July 24, 1995

Proceedings Editor
Christine H. Pennisi

Produced by the Illinois-Indiana Sea Grant Program, Phillip E. Pope Director. Illinois-Indiana Sea Grant is a joint federal and state program of Purdue University, West Lafayette, Indiana, and the University of Illinois at Urbana-Champaign. Funding is received from the National Sea Grant College Program, National Oceanic and Atmospheric Administration, and the U. S. Department of Commerce. The U. S. Government is authorized to reproduce and distribute reprints for governmental purposes notwithstanding any copyright that may appear.

Issued in furtherance of the Cooperative Extension Service of both Purdue University and the University of Illinois at Urbana-Champaign. Purdue University and the University of Illinois offer equal opportunities in programs and employment.

Production Coordinator, Nancy Riggs, Illinois-Indiana Sea Grant
Publication No. IL-IN-SG-97-6
For additional copies, contact Illinois-Indiana Sea Grant Communications 217 333-8055

CONTENTS

SEMINAR PROCEEDINGS:
WATER QUALITY APPLICATIONS OF SATELLITE REMOTE SENSING

Preface

A seminar was held on July 24, 1995 in downtown Chicago to explore water quality applications of satellite remote sensing. Although Lake Michigan water quality has improved significantly in the past three decades, concerns remain about the quality of this complex resource. Technology is rapidly evolving, and remote sensing has become a more accessible environmental monitoring tool. The following technical changes have raised the viability of using remote sensing as a monitoring tool:

1. Different types of imagery are available now, and more are coming on line each year, particularly from the international community.

2. This increased imagery availability and resultant competition among firms offering it will lower costs.

3. Software to analyze the imagery is getting more user friendly, with a wide range of choices and increased competition that also lowers costs.

4. The prevalent usage of GIS in environmental management agencies makes the imagery more useful because combined with many other layers of data, imagery is often complementary, i.e., it adds more spatial data that helps the user obtain an even truer picture of the location that is being studied.

5. GPS makes geo-correcting imagery easier and faster.

6. The federal government is being pushed by users and potential users of this data to make this type of tax-supported program more accessible through many routes including providing funding for the usually expensive imagery and its processing.

7. Experimental use of remote sensing has progressed for over two decades, so this tool has a solid research and expert personnel base from which to draw.

8. With government dollars shrinking and demand for environmental protection increasing, faster, cheaper, yet accurate data collection is needed as a basis for decision-making; remote sensing is one tool that can meet that need.

The purpose of this seminar was to: 1) inform water quality managers in Illinois and Indiana of the increasing potential of using remote sensing to monitor Lake Michigan water quality parameters; and 2) increase the interaction of these managers with experts in the field.

Formal presentations covered nonpoint source pollution; optically active water quality constituents; detecting interruptions in wastewater dissipation; and recommendations on ways that remote sensing can add to water quality decision making. These topics were enhanced by an informal exchange between speakers and participants throughout the remainder of the workshop.

Identifying Potential Non Point Source Pollution with Remote Sensing and GIS

Presentation by Wilma Subra, Subra Co., Inc.

Seminar on Water Quality Applications of Satellite Remote Sensing
Illinois - Indiana Sea Grant Program
Cooperative Extension Service
University of Illinois
July 24, 1995

Background

Pollutants that are discharged into surface waters from Point Sources such as pipes and channels are regulated under the Clean Water Act. The facilities with Point discharge Sources are required to have federal and state discharge permits. In Louisiana, the state does not have primacy for the NPDES program, thus facilities are required to have a Louisiana Water Discharge Permit System (LWDPE) permit and a Federal National Pollutant Discharge Elimination System (NPDES) permit.

Over the past 15 years, the Point Source program has greatly reduced pollutant loading in the surface waters of the United States. However, surface water quality problems still exist and the leading cause of surface water quality impairment is storm water runoff from Non Point Sources. Section 402(p) of the Water Quality Act of 1987 (WQA) requires the establishment of a comprehensive two-phased approach for the control of storm water runoff. Phase I regulations cover storm water discharges associated with industrial activities and municipal storm sewer systems serving a population of 100,000 or more. All Phase I industrial and municipal facilities are in the initial stages of the NPDES permitting process. Phase II regulations are being drafted and will cover all storm water discharges not addressed under Phase I.

Under section 319 of the Clean Water Act, a program was also established to control Non Point Sources of water pollution. The individual states are required to assess Non Point Source Pollution problems within their state, adopt management programs to control Non Point Pollution and implement the management plans. One of the first phases of assessing Non Point Sources of Pollution in each state is the identification of land cover which may contribute significantly to the degradation of surface water resources.

Objective

In order to identify areas of prime Non Point Source concern, a method was developed to use remotely sensed imagery and GIS modeling techniques to produce a generic model. The model was designed to identify, quantify and prioritize areas of Non Point Pollution contribution potential within a water quality basin area. The initial phase of this study performed as part of a Visiting Investigator Program at NASA's Stennis Space Center in Mississippi.

Study Area

The Calcasieu River Basin in southwest Louisiana has been impacted by Non Point Source Pollution and contains a wide variety of land cover types. The study area is a 20 mile by 20 mile section of the Calcasieu River Basin, which drains a total of 3,775 square miles. The study area is located approximately 15 miles inland and north of the Gulf of Mexico. The boundaries of the study areas were established in order to include known land covers of various types within the river basin. The habitats include: saline, brackish, intermediate, and fresh water marsh; prairie terrace; and upland forest. The land cover types include: agriculture, urban, commercial, light industry, heavy petrochemical refining industry, forest, pasture, swamp and marsh wetlands, rivers, streams, open bays, lakes, and an estuary system.

The entire Calcasieu Estuary system has been impacted by the industrial discharges from the Lake Charles Petro Chemical Complex. The industrial runoff of priority organics, non priority organics and metals has impacted the sediments and aquatic organisms along a 37 mile stretch of the Calcasieu River and Ship Channel, 1114 acres of Lake Charles, 1084 acres of Prien Lake, 67 square miles of Calcasieu Lake, 6 miles of Bayou D'Inde and 5 miles of Bayou Verdine. The sediments are contaminated with hexachlorobenzene, hexachlorobutadiene, PCB's, 1,2-dichloroethane, bromoform, halogenated aliphatics, aromatic priority pollutants and heavy metals such as mercury.

In 1987 the state agencies issued an advisory on consumption of any seafood on part of the river system, Bayou D'Inde and Prien Lake. In 1989 the advisory was extended to the entire estuary system for spotted sea trout and sand sea trout. In 1990 a number of species were added to the advisory - blue catfish, sea catfish, yellow bass, southern flounder and spot.

The study area consist of all or parts of eight Watersheds within the Calcasieu River Basin (Table 1). The designated uses are primary and secondary contact recreation and propagation of fish and wildlife. The designated uses range from being in full compliance to being in non-compliance (Table 2). Seven of the eight Watersheds are being impaired by Non Point Source Pollution.

The causes of Non Point Pollution in the study areas of the Calcasieu River Basin are:

- organic enrichment
- salinity
- total dissolved solids
- priority organic pollutants
- phenol
- non-priority pollutant organics
- heavy metals
- nutrients
- pesticides
- pathogens
- oil
- grease
- halogenated aliphatic and aromatic organic priority pollutants.

The major sources of Non Point Pollution in the study areas of the Calcasieu River Basin are:

- agricultural runoff
- urban runoff
- municipal runoff
- industrial runoff
- forestry runoff
- pasture land
- petroleum activities
- unsewered areas
- irrigated and non-irrigated crop production
- silviculture
- construction
- resource extraction
- land disposal
- hydromodification

Remote Sensing and GIS Data

1. Land Cover

The mapping of land cover that affects surface water quality enables the identification of areas with the highest pollution potential. A February 8, 1993 Landsat Thematic Mapper (TM) scene was used to develop a land cover classification. The ERDAS 7.5 program CLUSTR was used with TM bands 2, 3, 4, and 5 and the number of classes parameter set to 63 to develop a land cover classification. Default values were used for all other input parameters. The first iteration of CLUSTR yielded 63 classes. Although 1 signature from the

CLUSTR routine should represent 1 land cover type, confusion occurred in 4 of the resulting signatures. These signatures were further broken down into 10 signatures using MASK to extract the raw data followed by CLUSTR to develop 10 signatures with the distance parameter set to 1 for each mixed class. For each mixed class, this breakdown produced 2 distinct homogeneous classes with the remaining 8 still mixed but now a minority. The 40 new classes were grouped into land cover classes. The ERDAS 7.5 Program STITCH was then used to incorporate the new classes into the classification. The 103 resulting classes were then reduced to 15 land cover types.

Class Number	Land Cover Type
1	Open Water
2	Shallow Water
3	Industrial/Commercial
4	Heavy Industrial
5	Agricultural
6	Wetland Vegetation
7	Residential
8	Agricultural/Residential/Wetland Mix
9	Bare Soil
10	Scrub/Shrub
11	Upper Wetland Grasses
12	Coniferous Forest
13	Deciduous Forest
14	Bottom Land Hardwoods
15	Coniferous/Deciduous Mix

Because of the higher spatial resolution of SPOT data, a December 10, 1990 panchromatic scene was purchased to assist in delineating heavy industrial complexes. This process incorporated on screen digitizing to improve the accuracy of the model within these heterogeneous areas.

Both the TM and SPOT images were rectified and georeferenced to the Universal Transverse Mercator (UTM) projection with less than 30 meter pixel Root Mean Square (RMS) error accuracy. The heavy industrial complexes were digitized in the SPOT image and merged into the TM image to more accurately depict the heavy industrial complexes.

A model was developed to incorporate Remote Sensing and GIS data along with various physical and chemical parameters to produce a Non Point Source Pollution Model (Figure 1). The major inputs into the model are land use or land cover, soil types, slope and distance to water. In order to be of utility in the model, the land cover types had to be weighted according to contribution to Non Point Pollution.

The land cover classifications were then weighted on a scale of 1 to 20 ranging from low to high contribution potential for Non Point Source Pollution (Table 3). The weights assigned in this phase as well as the other phases of the project were based on technical knowledge and field experience. The development of ranking systems in models is an iterative process. Changes to the ranking system can be made to accommodate area specific and discipline specific applications.

Land Cover Category #	Description	Model Weight
1	Open Water	2
2	Shallow Water	2
3	Industrial/Commercial	17
4	Heavy Industrial	20
5	Agricultural	10
6	Wetland Vegetation	1
7	Residential	13
8	Agricultural/Residential/Wetland Mix	8
9	Bare Soil	10
10	Scrub/Shrub	4
11	Upper Wetland Grasses	1
12	Coniferous Forest	7
13	Deciduous Forest	5
14	Bottom Land Hardwoods	1
15	Coniferous/Deciduous Mix	6

The wetland vegetation (#6), upper wetland grasses (#11), and bottom land hardwoods (#14) classes were assigned the lowest possible weight of one because these classes benefit the Watershed by reducing some of the pollution through absorption before it enters the water body. All rainfall in the study areas is likely to be contaminated by the absorption of pollutants from the local atmosphere, but rainfall interacting with the wetlands environment is filtered by numerous chemical reactions, such as organic mineralization reactions and inorganic cation exchange reactions. Precipitation falling in open or shallow water has no opportunity to interact with any filtering process prior to entering the surface water body. Therefore, the open water (#1) and shallow water (#2) classes were assigned a slightly higher weight of two.

At the other end of the weighting scheme, heavy industry (#4) was ranked as a 20 because of the abundant impervious surfaces and extreme pollutant loading. The field evaluation supports the high ranking. The industrial/commercial (#3) class was weighted at 17 in order to represent its slightly lesser contribution to Non Point Source Pollution. The residential (#7) class was assigned a relatively high weight of 13 because it represents a large amount of impervious surfaces, such as streets, driveways, and roofs, and causes of Non Point Source Pollution, such as oil, grease, and residential pesticides.

The agricultural (#5) class was weighted 10 because of the pesticide and herbicide use in south Louisiana. Bare soil (#9) was weighted 10 because it is essentially an impervious surface in terms of runoff potential and its large contribution to total suspended solids (TSS) and total dissolved solids (TDS). The agricultural/residential/wetland (#8) mixed class was weighted 8, which is slightly lower than agricultural, to represent the wetlands portion of the class.

Managed forests have a large input of pesticides and herbicides to Non Point Source Pollution. Forest canopies also intercept relatively large amounts of aerosol pollutants via atmospheric deposition. These pollutants are washed off during the first flush of a rainfall event. Because the deciduous canopy was sparse when the TM data was acquired in February, coniferous forest (#12) was weighted 7 to represent a greater contributor to Non Point Source Pollution. The deciduous forest (#13) was weighted 5 and the coniferous/deciduous mix (#15) was weighted 6.

The scrub/shrub (#10) was weighted 4. This class is a transitional land cover type falling between wetlands and the upland classes. It is better than the upland classes but not quite as effective as wetlands in filtering pollution.

Watersheds

Watershed boundaries were digitized from a Water Quality Management Basins Map acquired from the Louisiana Department of Environmental Quality, Office of Water Resources. The study area contains all or part of eight Watersheds. These Watersheds varied widely from Bayou drainage systems to River drainage basins to a large lake to bay estuary system. Each of these 8 Watersheds was assigned a unique number from 1 through 8 (Table 1). The Watershed boundaries were useful in creating a "distance to water" layer within each Watershed and were useful in restricting statistics to individual Watersheds.

Hydrography

A hydrography layer was developed from 1:100,000 United States Geologic Survey (USGS) Digital Line Graph (DLG) data. The DLG provided better identification of small streams and canals than did the image classification but failed to delineate local wetland boundaries. For this reason, known wetlands from the land cover classification were added to provide more accurate delineation of open water bodies. The Watershed and hydrography layers were then joined together to permit distance to water calculations by individual water shed.

Distance to Water

A distance to water routine was used to measure the distance to water within each individual Watershed. With the maximum distance to water set to 254 pixels, the distance

layer extended beyond the boundaries of each Watershed. The distance layer was clipped to each Watershed boundary by multiplying by the appropriate Watershed set to 1 and all other Watersheds set to 0. The resulting eight distance layers were then put together into one layer.

For input into the model, the distance to water layer was ranked from 1 to 20 based on how far from water a given location fell. The ranks were assigned in increments of 7 pixels, representing 210 meters. Locations from 0 to 210 meters from water were ranked the highest while locations greater than 3,990 meters distance from water were ranked the lowest. Locations nearer water have a higher ranking because these locations potentially contribute more NPS Pollution to waterbodies than those locations further away.

Distance	Rank	Distance	Rank	Distance	Rank
0 to 210	20	1,471 to 1,680	13	2,941 to 3,150	6
211 to 420	19	1,681 to 1,890	12	3,151 to 3,360	5
421 to 630	18	1,891 to 2,100	11	3,361 to 3,570	4
631 to 840	17	2,101 to 2,310	10	3,571 to 3,780	3
841 to 1,050	16	2,311 to 2,520	9	3,781 to 3,990	2
1,051 to 1,260	15	2,521 to 2,730	8	>3,990	1
1,261 to 1,470	14	2,731 to 2,940	7		

Slope

USGS Digital Elevation Model (DEM) data were not available at any scale for this study area. To obtain elevation data, the contours on 1:62,500 quad sheets were digitized. From the digitized contours, elevation and slope were derived using TOPO.

For this model, the slope layer was ranked from 1 to 20 based on percent slope. The ranks were assigned in 5% increments which represents 2.25° of slope. Slopes from 0 to 5% (0 to 2.25 degrees) were ranked the lowest and the slopes greater than 95% (42.75 degrees) were ranked the highest. One hundred percent slope represents a 45° slope. The greater the slope, the more quickly water drains through the area, increasing its impact on NPS Pollution.

Soil Permeability

Soil types were digitized from 1:316,800 United States Department of Agriculture (USDA) General Soil Maps. The types were grouped into 4 categories: poorly to moderately well drained soils were assigned a model weight of 6; poorly drained soils, weighted 9; very poorly drained soils, weighted 12; and open water, weighted 0.

Pollution Potential Model

Using the ERDAS Imagine Spatial Modeler, the ranked land cover, soil type, slope and distance to water layers were input to the model. The layers were added together, producing a sensitivity layer ranging from 9 to 80. The higher numbers indicate the locations more likely to contribute to Non Point Source Pollution. The range of values was divided into 13 equal classes which were "painted" various colors using software in order to produce the display. The blues and greens designate areas of low Non Point Pollution potential. The yellow to orange areas are of moderate potential and the red to magenta designated areas are high Non Point Pollution potential.

In order to evaluate the potential impacts of Non Point Source run off to existing water quality, the Watersheds were ranked from 1 through 20 based upon their compliance with designated water uses (Table 2). The compliance is established every two years by the Louisiana Department of Environmental Quality as part of their requirements under the Clean Water Act, Section 305 (b). Watersheds 2 and 6 were in full compliance and rated 4. Watersheds 1 and 8 ranged from threatened to full compliance and were rated 10. Watersheds 5 and 7 were threatened and rated 14. Watershed 4, ranging from threatened to non compliance, rated 16 and Watershed 3 was in non compliance and rated 18. The output of the Non Point Source Pollution Potential Model was then combined with the weighted Watershed compliance of designated uses to produce the Non Point Source Pollution impact layer. The addition of the ranked Watershed layer produced a sensitivity layer ranging from 13 through 98. Once again, the higher numbers indicated locations most likely to contribute to Non Point Source Pollution. The values were painted to produce the image. Once again low pollution impact areas are blue and green, moderate are yellow to orange and high are red to magenta.

The majority of locations in Watersheds 2, 5 and 7 were shifted towards the low end of the sensitivity range, indicating less of a priority because the Non Point Source Pollution in these Watersheds will have less of an impact on surface water quality. Watersheds 1, 3, 4, 6 and 8 remained high in Non Point Source Pollution potential and therefore are a priority for the control of Non Point Source Pollution.

The land cover classifications were subjected to a statistical routine. The outputs determined various land cover categories in each water shed. The total acreage in each Watershed was calculated (Table 1). The land cover categories in each Watershed by acreage and percent were compiled (Table 4). Statistics representing the pollution potential within each Watershed were calculated from the output of models 1 and 2. The results were printed out for each Watershed for both models.

The Watershed with the lowest potential for Non Point Source Pollution was Watershed V (Table 5). This Watershed was the area known as Calcasieu Lake. The Watershed contained 53% open water, 4% shallow water, 22% wetlands and 9% agriculture. The designated water uses are threatened by upstream sources and surface runoff.

Watershed III had the highest Non Point Source Pollution potential and impact (Table 6). This Watershed consist primarily of industrial and commercial facilities, and agricultural land use. The Watershed does not meet its designated uses and is being impacted by petrochemical industrial facilities, industrial and municipal storm sewers, surface runoff, and Non Point Sources. This Watershed known as Bayou D'Inde is currently posted with a fish advisory that limits consumption to two meals a month and a swimming advisory which prohibits swimming and contact with the contaminated sediments. The pollutants in the sediments and aquatic organisms are hexachlorobenzene, hexachlorobutadiene and PCB's from an industrial Point Source. The EPA is currently evaluating Bayou D'Inde as a potential superfund site.

Conclusion

The application of remote sensing and GIS techniques in the identification of areas of Non Point Source Pollution potential is extremely useful. The remote sensing data served as a very valuable tool in the identification and classification of current land cover categories. Periodic updates of data enable evaluation over time as well as the evaluation of the effectiveness of projects. The software programs provided statistics on the quantity of each land cover type within a specific area. The remote sensing and GIS techniques are excellent tools for providing the various layers which are incorporated into the Non Point Source Pollution potential models. This model represents site specific as well as Watershed composite data on the potential of Non Point Source Pollution. When the model is executed in conjunction with surface water quality data, the areas with the highest potential for Non Point Source runoff impacting surface water quality are delineated. These are the areas where the greatest impact of improving surface water quality could be realized from the implementation of Best Management Plans. These are the areas that should be addressed first when developing best management strategies for Non Point Source Pollution control.

The techniques developed as a part of this study have demonstrated that remote sensing and GIS techniques provide an effective and efficient means of providing data necessary for Non Point Source Pollution management. The data will enable federal, state and local agencies to assess Non Point Source Pollution issues by identifying:

- land cover types that are major contributors in Non Point Source Pollution
- specific areas where these land cover types have the highest potential for providing polluted runoff
- areas where the Non Point Source runoff has the highest potential for impacting the receiving water bodies

The techniques will provide agencies and industries with the tools necessary to perform the following functions:

- develop appropriate management measures for sources of Non Point Pollution
- estimate the cost of various management measures
- determine the effectiveness of implemented management measures
- prioritize spending to concentrate resources on implementing plans that will result in the reduction of significant pollution.

Table 1

Calcasieu River Basin Watersheds

Watershed #	Segment	Description	Acre
I	0308	West Fork of the Calcasieu River	25,692.334
II	0310	Bayou Choupique	22,842.697
III	0309	Bayou D'Inde	20,344.232
IV	0303	Ship Channel and Estuary	52,525.594
V	0304	Calcasieu Lake	68,974.227
VI	0311	Intracoastal Waterway	107,816.758
VII	0302	Upper Calcasieu River	6,832.415
VIII	0307	English Bayou	22,986.902

Table 2

Watershed	Degree of Support of Designated Water use	Model Weight
I	Threatened/Full Compliance	10
II	Full Compliance	4
III	Non-Compliance	18
IV	Threatened/Non-Compliance	16
V	Threatened	14
VI	Full Compliance	4
VII	Threatened	14
VIII	Threatened/Full Compliance	10

NONPOINT SOURCE POLLUTION MODEL

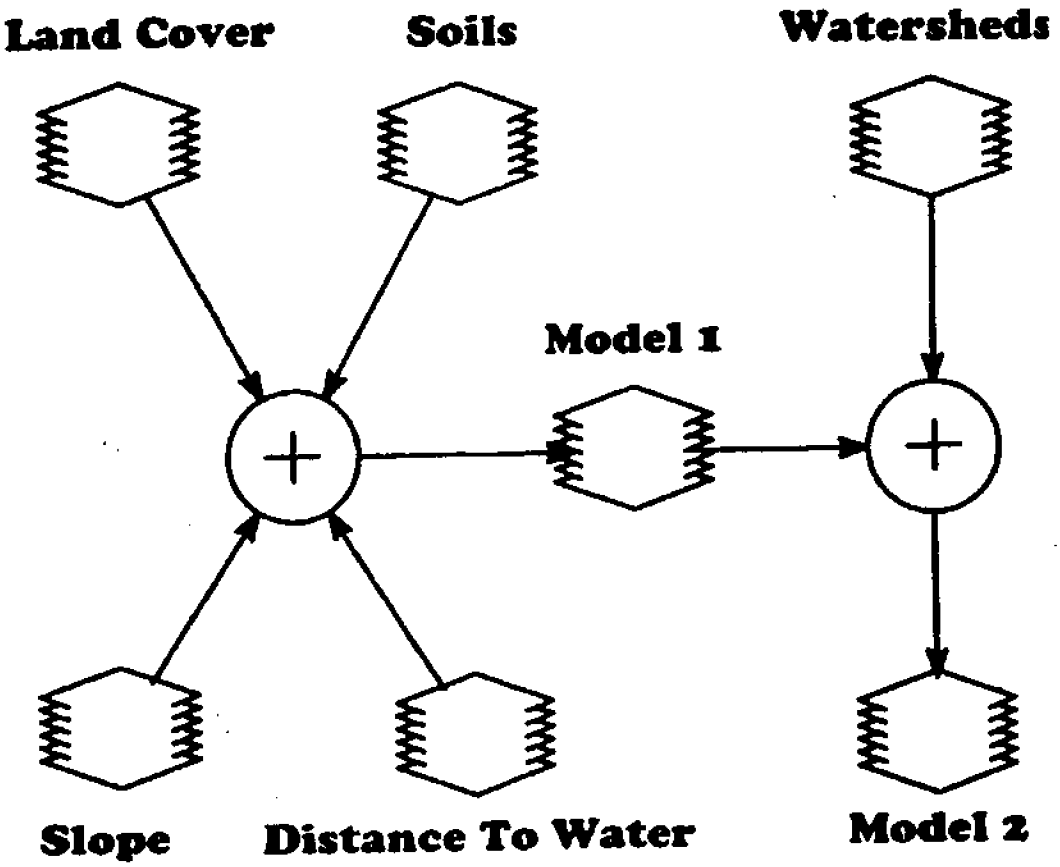

NASA Office of Advanced Concepts & Technology
Commercial Remote Sensing Program Office
Stennis Space Center

SUBRA COMPANY

Figure 1

Table 3

LAND COVER TYPES

[illegible]	Land Cover	[illegible]	Acreage
6	Wetland Vegetation	1	12,043.70
11	Upper Wetland Grasses	1	5,637.20
14	Bottom Land Hardwood	1	2,209.30
1	Open Water	2	21,769.80
2	Shallow Water	2	4,838.10
10	Srub/Scrub	4	29,615.50
13	Deciduous Forest	5	2,359.00
15	Conif./Deciduous Mix	6	17,433.20
12	Coniferous Forest	7	1,599.50
8	Agric./Resid./Wet Mix	8	45,551.10
5	Agriculture	10	64,553.50
9	Bare Soil	10	2,256.50
7	Residential	13	8,910.80
3	Industrial/Commercial	17	7,556.30
4	Heavy Industry	20	6,871.80
	TOTAL ACREAGE		233,205.30

Table 4

Land Cover Categories in Watershed I
Waterbody Segment 0308
West Fork of the Calcasieu River
in the Calcasieu River Basin

#	Land Cover Category Description	Acres	Watershed
1	Open Water	459.893	1.79%
2	Shallow Water	128.462	0.50%
3	Industrial/Commercial	483.016	1.88%
4	Heavy Industrial	0.000	0.00%
5	Agricultural	4,449.912	17.32%
6	Wetland Vegetation	1,610.909	6.27%
7	Residential	852.985	3.32%
8	Ag/Residential/Wetland Mix	4,103.066	15.97%
9	Bare Soil	154.154	0.60%
10	Scrub Shrub	5,580.375	21.72%
11	Upper Wetland Grasses	698.831	2.72%
12	Coniferous Forest	734.801	2.86%
13	Deciduous Forest	644.878	2.51%
14	Bottomland Hardwoods	115.616	0.45%
15	Coniferous/Deciduous Mix	5,675.437	22.09%

Table 5

Potential for Contribution to
Nonpoint Source Pollution in
Watershed V
Waterbody Segment 0304

Potential for Contribution to Nonpoint Source Pollution		Model 1		Model 2	
		Acres	%	Acres	%
Low	1	23464.088	34.02		
	2	1669.260	24.17		
	3	1895.978	2.75	38524.937	55.85
	4	1107.340	1.61	2984.414	4.33
	5	637.404	0.92	1627.316	2.36
	6	6366.260	9.23	1045.290	1.52
	7	5449.741	7.90	8600.733	12.46
	8	6878.229	9.97	8015.149	11.62
	9	3644.058	5.28	5314.521	7.71
	10	1293.935	1.88	1496.544	2.17
	11	770.401	1.12	853.802	1.24
	12	491.731	0.71	416.337	0.60
High	13	305.803	0.44	95.188	0.14

Table 6

Potential for Contribution to
Nonpoint Source Pollution in
Watershed III
Waterbody Segment 0309

Potential for Contribution to Nonpoint Source Pollution		Model 1		Model 2	
		Acres	%	Acres	%
Low	1	118.985	0.58		
	2	115.204	0.57		
	3	306.915	1.51	73.393	0.36
	4	787.081	3.87	129.216	0.64
	5	2359.464	11.60	338.496	1.66
	6	3622.930	17.81	1159.160	5.70
	7	4549.680	22.36	3657.180	17.98
	8	2903.459	14.27	5373.012	26.41
	9	1939.569	9.53	4033.262	19.82
	10	2063.891	10.14	2455.319	12.07
	11	862.475	4.24	2041.206	10.03
	12	385.645	1.90	691.671	3.40
High	13	328.933	1.62	392.317	1.93

A REVIEW OF REALIZED AND POTENTIAL SUCCESSES OF REMOTE SENSING OF THERMAL AND OPTICAL FEATURES OF LAKE MICHIGAN

David Bolgrien
Center for Limnology & Environmental Remote Sensing Center
University of Wisconsin-Madison

Abstract

The potential of lake surface temperature data, especially those derived from satellites, has been realized in limnological research. However, the potential of remotely sensed optical data remains less straightforward. The first case-study shows that the major thermal features of Lake Michigan (i.e. the migration of vernal thermal fronts, upwelling, and the seasonal temperature cycle) may be delineated successfully on a multi-season, whole-lake basis using daily satellite imagery with 1 km pixels and a 0.5°C temperature resolution. The second case-study describes wavelength-specific absorption spectra for chlorophyll, dissolved organic matter, and suspended solids measured along the trophic gradient of Green Bay. These data link spectral reflectance and component concentrations but their variabilities must be better understood before bio-optical models may be considered operational.

Introduction

Remote sensing techniques have long been successfully applied in oceanography and terrestrial ecology, but the same is not true for limnology. The reasons for this situation are diverse but largely result from the difficulty of linking limnological variables with radiometric data through appropriate calibration studies or models. Validating and calibrating linkages is challenging in lakes because water quality is highly dynamic in space and time, and ubiquitous optical complexity imparted by allochthonous inputs and proximity of sediments. It is assumed that remotely-sensed data, systematically collected over a wide area, will improve our understanding of physical and biological processes in lakes. Two case-studies presented here demonstrate the technical and limnological realities of this assumption.

In the first case-study, satellite-derived water temperatures are used to delineate thermal and hydrodynamic features of Lake Michigan. The operational determination of lake surface temperatures exemplifies the realized potential of satellite remote sensing. In the second case-study, absorption spectra of chlorophyll, dissolved organic matter, and particles in Green Bay (Lake Michigan) are compared to other lakes. Bukata *et al.* (1995) advocate that understanding component optical properties is a necessary, but insufficient, step towards modeling component concentrations from satellite optical data - arguably the ultimate goal of oceanic and limnological remote sensing. This goal remains elusive.

In the open oceans, where chlorophyll *a* is the major optically-active component, concentrations may be determined by the blue:green reflectance ratios (Gordon *et al.*

1988). Optical properties and spectral reflectance are linked by the characteristic shape of the chlorophyll absorption spectra. Additional optically-active components, common in lakes and coastal marine environments, confound this strategy. Many limnological remote sensing studies have bypassed the investigation of fundamental optical properties to pursue empirical linkages between water quality and spectral reflectance. It has became clear that empirical approaches have limited utility because equations are only valid for the place and time of sampling. Extrapolation of reference (or 'ground-truth') data over large areas is inappropriate because of atmospheric interference, variable viewing/solar geometries, and heterogeneities in the optical properties of the lakes themselves (see Lathrop and Lillesand 1986, 1987, 1989; Lathrop *et al.* 1990). The Green Bay case-study shows that optical properties contributing to spectral reflectance vary across the bay.

Remotely-sensed data must be available at spectral, temporal, and spatial scales relevant to the feature investigated and research question posed. The design of sensors has been a series of trade-offs among spatial, spectral, and temporal resolutions. Aircraft-based sensors offer quite flexible resolutions but cannot provide economical long-term, wide-area coverage. Satellite-based sensors can provide such coverage but only at fixed spatial and temporal resolutions. For example, the dynamics of thermal features of the Great Lakes are evident using >daily satellite images with a pixel size of 1 km of the Advanced Very High Resolution Radiometers (AVHRR) (Mortimer 1988; Bolgrien and Brooks 1992; Bolgrien *et al.* 1995b). It would be difficult to detail these dynamics using the Landsat Thematic Mapper because of its 16 day revisit frequency. The Coastal Zone Color Scanner (CZCS) (Tanis 1984), and its eventual replacement, the Sea-viewing Wide-Field-of-view Sensor (SeaWiFS), were specifically designed for biological oceanography research by the inclusion of several narrow visible bands.

Realized Success:

Thermal features of Lake Michigan derived from satellite-measured surface temperatures

The distribution of heat in a lake is a product of seasonal solar inputs, morphometry, river inflows, internal motions, and interactions between the water and the atmosphere. Resultant thermal features include seasonal heating and cooling cycles, the formation and migration of vernal thermal fronts, upwelling, and exchanges between the lake and bays. These features are directly related to key hydrodynamic properties and indirectly influence biological processes by controlling the distribution of organisms and nutrients. Satellite remote sensing is the latest in a succession of methods used to measure temperatures in Lake Michigan. It should not be considered, however, the best method. The greatest difference among these methods is their ability to depict spatial aspects.

Classical studies by Church (1945) and Mortimer (1968 & 1971) employed bathythermograph casts from trans-lake ferries to construct comprehensive three-dimensional views of the thermal structure of Lake Michigan. They unequivocally documented the formation of vernal thermal fronts, and the relationship between upwelling

and wind history. However, transect data could not represent the spatial dynamics of temperature of the entire lake. Nearshore temperatures recorded at municipal and industrial water intakes in Lake Michigan have been used to demonstrate the progression of Kelvin waves and currents (Mortimer 1971). Daily mean temperature data from the Milwaukee, WI. intake demonstrate the unimodal seasonal temperature cycle of Lake Michigan (Figure 1). Major features include minimum temperatures in February, the onset of thermal stratification in April, and maximum temperatures in early September. Summer temperature fluctuations result from movement of the thermocline. Offshore water temperature and meteorological data for the Great Lakes are available through the NOAA National Data Buoy Center (NDBC). Eight NDBC buoys are deployed in the Great Lakes (two in Lake Michigan) (Lesht and Brandner 1992). These data demonstrate some of the spatial variability in the seasonal temperature cycle of the Great Lakes (Figure 2). For example, temperatures in southern Lake Michigan were consistently higher and thermal stratification began 10-20 days sooner than in northern Lake Michigan.

Water temperature measured by thermal scanners is derived from emitted long-wave (or thermal) infrared (IR) radiation (3,000 - 13,000 nm). The low thermal conductivity of water limits emission of long-wave radiation to <50 nm depth. Therefore, thermal scanners measure skin , or sea surface temperature (SST), a term which has been adopted for lakes. Heat fluxes at the air-water interface, particularly evaporation, cause SST to be typically $0.5^{\circ}C$ lower than temperatures in the upper few meters (or bulk temperature) (Schluessel *et al.* 1990). This limitation must be considered when interpreting lake surface temperature data derived from thermal scanners.

Airborne thermal IR scanners have been used to show the coincidence of SST and water color gradients in Lake Michigan (McFadden and Ragotzkie 1963; Noble and Wilkerson 1970). Flights over Lake Ontario detected thermal fronts, internal wave patterns, and small eddies (Lane 1970). The thermal plume of the Detroit River was mapped by Beeton *et al.* (1969). Scarpace *et al.* (1979) used multiple flights to delineate the Keweenaw current and upwelling in Lake Superior. The expense of frequent flights and navigation errors are cited liabilities in these studies.

A compromise between operational continuity and spatial scales for the remote sensing of Lake Michigan temperature was achieved in the AVHRR. Multiple sensors and a twice daily revisit frequency resulted in approximately 2-6 of the 14 images collected over Lake Michigan each week being suitably cloud-free for analysis (Bolgrien 1993). The AVHRR has visible (580-680 nm), near-IR (720-1,100 nm), mid-IR(3,500-3,900 nm), and two thermal IR (10,300-11,300 nm & 11,500-12,500 nm) bands. SST images of Lake Michigan are available through the NOAA CoastWatch Program via the Great Lake Environmental Research Laboratory (Schwab *et al.* 1992; Maturi and Taggart 1993; Leshkevich *et al.* 1993). The operational production of CoastWatch SST imagery systematically converts raw AVHRR data into SST using the current best algorithm. When a better algorithm becomes available, it is subsequently applied until it too is

replaced. There is no provision for the retrospective application of new algorithms to old data. Apparent changes in absolute SST must be interpreted in the context of changing algorithms. Metadata document changes in data processing, algorithm, and sensor calibration (Leshkevich *et al.*1993). The minimum detected SST difference is 0.5°C (Schwab *et al.* 1992). Temperature data may be aggregated and color-coded. Ice, clouds, and land may be masked by assigned a value of 255 (or white, <-5°C) or 0 (or black, >30°C). The major thermal features of Lake Michigan (1990-1993) are presented below using the results of Bolgrien (1993).

The annual cycle of median SST (representative of overall lake temperature on a given date) for Lake Michigan is monotonic with winter minima of <2°C reached in February/March and summer maxima of 19-24°C in September (Figure 3). Inter-annual variability in median SST is higher in the late spring and summer and lower during autumnal cooling. This is characteristic of the relatively rapid cooling of the epilimnion at fall turnover. SST frequency histograms of cloud-free pixels show heterogeneous distributions of SST values in the spring and fall as regions of the lake gain or lose heat (Figure 4). Summer and winter temperatures are relatively homogeneous. Limnological spring is evident as the SST frequency distribution and model value shift to warmer temperatures. The lake reaches its maximum heat content in August/September, and the variability of SST decreases (Figure 4b).

Spatial aspects of the temperature cycle of Lake Michigan are best demonstrated using whole-lake SST images (Figure 5). Winter conditions, with uniform SST of <5°C and ice in Green Bay and northern Lake Michigan, occur in February/March. In April, bands of warm water (>5°C) form near-shore, especially in the southern basin. These bands increase in width along the shore and migrate to the north through May. By late May, surface temperatures <5.0°C are confined to small patches in the northern basin. Green Bay consistently contains the warmest water in the lake during the ice-free season. Summer SST peaks in August/September after which SST begins to decrease across the lake.

The migration of the vernal thermal front in southern Lake Michigan was documented by plotting the position of the 5°C isotherm from SST images (Figure 6). In April/May, the 5°C isotherm appears 5-20 km from shore. The front begins a general offshore and northward migration. Brief shoreward retreats are possible, especially towards the southern end of the lake, but limnological spring typically occurs throughout the lake by mid-June. For example, in 1992 the total area of the lake located offshore of the 5°C isotherm (limnological winter conditions) decreased from 72% to 43% to 12% to 0% on 24 May, 28 May, 2 June, and 11 June, respectively.

Upwelling (vertically displaced metalimnetic water) is limnologically significant because of short-term nutrient enrichment of surface waters and the redistribution of plankton. However, the spatial and temporal dynamics of upwelling in Lake Michigan was not well known. AVHRR SST images in August and September 1992 represent the typical

upwelling pattern, as the wind was primarily from the south and southwest (Figure 7). Upwelling was most prevalent along the western shore of the lake, particularly along the Door Co. (Wisconsin) Peninsula. Surface temperatures in upwelling regions were generally $<20°C$ bands adjacent to $>20°C$ water offshore.

Water mixing between Green Bay and Lake Michigan was observed in AVHRR SST imagery (Figure 8). On 14 June 1990, a plume of Green Bay water transported through the Sturgeon Bay canal is evident as a mass of warm water ($>14°C$) along the Door Peninsula (Figure 8a). A similar plume was present on 26 June across the mouth of the bay as warm bay water mixing into the cooler waters ($<12°C$) of northern Lake Michigan (Figure 8b). Typically, little water leaves the bay through the canal compared to the mouth (Gottlieb *et al.* 1990).

Interactions between Lake Michigan and its tributaries have also been analyzed using satellite SST data (Lathrop *et al.* 1990). Mortimer (1988) observed bands of colored water in CZCS images extending along the eastern shore of Lake Michigan in spring. He hypothesized that these bands resulted from the trapping of allochthonous dissolved organic matter between the shore and the thermal front. Indeed, Moll *et al.* (1993) found that inputs from the Grand River, one of the largest tributaries to Lake Michigan, significantly contributed to near-shore warming along the eastern shore. However, river plumes were not apparent in AVHRR SST images (Bolgrien 1993) possibly because they rarely extend >3 km (about 3 AVHRR pixels) from shore (Chambers and Eadie 1981).

It is clear that the synoptic view of large lakes afforded by satellites makes it possible to delineate the spatial and temporal dynamics of thermal features systematically and comprehensively. Linking thermal and hydrodynamic features is important for successful monitoring of large lake water quality. Emitted thermal radiation is easy to measure and interpret compared to reflected optical data. Properties which contribute to the apparent color of a water body are numerous and diverse. The energy received in the optical bands has been modified by two transits through the atmosphere and by reflectance from a mixture of optically-active agents in some volume of lake. A central task for limnological remote sensing is to relate that signal to biological and chemical processes.

Potential Success:

Absorption spectra for chlorophyll, particles, and dissolved organic carbon in Green Bay

Deriving water quality information from remotely sensed reflectance spectra is more difficult in lakes than in the open ocean because of their optical complexity. This has hindered the incorporation of chlorophyll mapping into lake monitoring studies (Bukata *et al.* 1991b). Spectral reflectance from a lake is linked to water quality by the absorption and scattering coefficients of individual optically-active components, specifically water, chlorophyll, dissolved organic carbon (DOC), suspended minerals. Knowledge of absorption coefficients of water and chlorophyll is sufficient for most oceanic bio-optical

models (Morel and Prieur 1977). These coefficients are wavelength-dependent values of scattering and absorption ascribed to a unit concentration of material ($m^{-1}/mg \cdot m^3$ or $m^2 \cdot mg^{-1}$) (Bukata *et al.* 1985). Absorption of light by a water body is equal to the sum of the products of absorption coefficients and concentration of each component or $a_{total}(\lambda) = a_{water}(\lambda) + a_{doc}(\lambda)[doc] + a_{particles}(\lambda)[particles] + a_{chl}(\lambda)[chl]$, where bracketed variables refer to concentrations. Since $a_{water}(\lambda)$ is known (Smith and Baker 1981), spectral variability in $a_{total}(\lambda)$ results from variations in $a_{doc}(\lambda)$, $a_{particles}(\lambda)$, $a_{chl}(\lambda)$ and their respective component concentrations. In lakes, scattering coefficients are typically insignificantly small relative to absorption and either decrease monotonically with wavelength or are spectrally neutral (Gordon *et al.* 1988; Gallie and Murtha 1992). Improvements to limnological bio-optical models are expected from better estimates of the magnitude and variabilities of absorption coefficients.

The magnitude and variability of $a_{doc}(\lambda)$, $a_{particles}(\lambda)$, and $a_{chl}(\lambda)$ were determined for Green Bay as part of the USEPA-sponsored Great Lakes Ecological Process Pilot Project in 1992 (Bolgrien *et al.* 1995b). Green Bay was attractive for limnological remote sensing research because it contains a wide range of trophic conditions in a relatively small area (Lathrop and Lillesand 1986, 1987, 1989; Lathrop *et al.* 1990; Lathrop 1992). The shallow eutrophic southern end of the bay is highly turbid with elevated concentrations of chlorophyll, particles, and organic carbon compared to the mesotrophic northern end (Sager and Richman 1991).

Total suspended solids, chlorophyll, and total and dissolved organic carbon were determined along the tropic gradient of the bay. Absorption spectra of particulate matter (which included chlorophyll) ($a_{particles}(\lambda)$) were determined spectrophotometrically using the quantitative filter technique (QFT) of Mitchell (1990). Absorption of light by dissolved organic carbon ($a_{doc}(\alpha)$), also measured spectrophotometrically, decreased exponentially with increasing wavelength. The spectral extinction coefficient for DOC (S as nm^{-1}), calculated as the slope of the semilog absorption between 400 and 550 nm, provided a means to compare $a_{doc}(\alpha)$ from different lakes. Absorption coefficients for chlorophyll, particles, and DOC were calculated at 14 wavelengths from measured component concentrations and measured absorption spectra using the bio-optical model of Bukata *et al.* (1995 and references therein). It was hypothesized that lakes of similar trophic status have similar optical properties. As this model has been applied to Lake Ontario, Lake St. Clair, Lake Ladoga, and Chilko Lake (Bukata *et al.* 1985, 1988, 1991a; Gallie and Murtha 1992, respectively), Green Bay results could be directly compared.

In Green Bay, mean and standard deviation spectra for particulate absorption ($a_{particle}(\lambda)$) were similar in shape (Figure 9) suggesting that $a_{particle}(\lambda)$ was highly variable throughout the bay, but spectra had the same basic shape. Chlorophyll absorption peaks at 435 nm and 675 nm were the major features. The region of 400-440 nm had maximum absorption values and variability which may be attributed to detritus (Roesler *et al.* 1989). Chlorophyll-specific absorption ($a_{particle}(\lambda) \cdot [chl]^{-1}$) and total suspended solids-specific

absorption ($a_{particle}(\lambda)\cdot[tss]^{-1}$) were calculated to remove the biomass signal. In both cases, the standard deviation spectra were reduced relative to the mean and retained the shape of the mean spectra. This showed that chlorophyll and total particle concentrations accounted for about the same portion of the overall spectral variance.

To further compare relative spectral shape, total absorption spectra were normalized to the mean value for the wavelength range measured ($a_{particle}(\lambda)\cdot(\sum a_{particle}(\lambda)/n)^{-1}$, where n=61 measured wavelengths). This eliminated biomass bias and artifacts of normalization at an arbitrary wavelength (Mitchell and Kiefer 1988). Standard deviation were greatly reduced and spectrally neutral with this normalization (Figure 9). The mean spectrum still showed absorption by chlorophyll *a*. These results were consistent with the oceanic data of Garver *et al.* (1994) who concluded that the quantity, not quality, of absorptive material explains most of the variability in the overall absorption signal.

Green Bay $a_{particle}(\lambda)$ values were highly variable in the blue portion of the spectrum (400-450 nm), and variability decreased with increasing wavelength (Figure 10). Green Bay $a_{particle}(\lambda)$ were similar to Chilko Lake and marine values (Gallie and Murtha 1992; Garver *et al.* 1994) but were significantly lower than those from Lake Ontario and Lake Ladoga. In general, $a_{particle}(\lambda)$ spectra had a U shape with minima near 570-600 nm. Particle characteristics presumably varied greatly between Green Bay and Chilko Lake because glacial flour in Chilko Lake lacked adsorbed organic matter and the phytoplankton component of $a_{particle}(\lambda)$ was relatively small (Gallie and Murtha 1992). Particles of Green Bay contained significant amounts of chlorophyll and derived from organic-rich sediments. The resulting $a_{particle}(\lambda)$ spectra had characteristics of the $a_{chl}(\lambda)$ spectra such as an absorption peak at 670 nm. Neither Gallie and Murtha (1992) or Green Bay results explained why such different particle types have such similar absorption characteristics.

Values of $a_{chl}(\lambda)$ values were highly variable in the blue (400-450 nm) (Figure 10). Almost the entire range of $a_{chl}(\lambda)$ values from other lakes was included in ± 1 sd of the mean Green Bay values. Since no range or variance information was available for other lakes, it was difficult to determine whether the Green Bay data were typical. Green Bay $a_{chl}(\lambda)$ values were very similar to those of Chilko Lake in the green. Differences between the four lakes diminished in the red (>600 nm) and most had a characteristic chlorophyll absorption peak near 670 nm (Figure 10). Literature comparisons with other water bodies showed similar variability in $a_{chl}(\lambda)$ values.

The mean exponential slope (S) of the $a_{doc}(\lambda)$ spectra for Green Bay was greater than published values for lakes and diverse marine waters (Bolgrien *et al.* 1995b). However, the variability in published values suggest their ranges may be relatively small. The spectral absorption coefficients of dissolved organic carbon ($a_{doc}(\lambda)$) in Green Bay and Chilko Lake $a_{doc}(\lambda)$ were relatively high in the blue and decrease with increasing wavelength (Figure 10). Differences among the four lakes were greatest in the blue and decreases with increasing wavelength. Green Bay $a_{doc}(\lambda)$ values were lower than Lake Ontario from 550-

700 nm. The mean Green Bay S value (0.020 $\pm$0.006 nm^{-1}) was higher than offshore Lake Ontario (0.009 nm^{-1}) and Lake Ladoga (0.006 nm^{-1}). The spatial distribution of variables influencing S in Green Bay was associated with the trophic gradient (Figure 11). Extinction was highest at eutrophic stations of southern Green Bay. Environmental influences on S and $a_{doc}(\lambda)$ may be related to the chemical composition and sources of DOC, such as humic and fluvic acids from allochthonous matter and decomposition of organic sediments.

Results for Green Bay demonstrate that inherent optical properties can be related to water quality variables in lakes. However, lakes with similar trophic characteristics can have very different optical properties and therefore spectral reflectance signatures. Bukata *et al.* (1991b) advocated that functional remote sensing limnological chlorophyll algorithms may require the determination of specific absorption coefficients for every optically-complex water mass. Absorption coefficients were more influenced by the concentration of particles rather than their spectral characteristics. In Green Bay, total suspended particle concentrations explain roughly the same amount of variance of spectral absorption as chlorophyll concentrations. However, sufficient variability remains unexplained to prevent a single set of optical coefficients from modeling reflectance in diverse lake types or even within a single lake. Bukata *et al.* (1991b) go so far as to advocate the quantification of the spatial, and even seasonal, variability of absorption coefficients in lakes at a global scale before remotely-sensed data may be utilized in limnological research. It is unlikely that a single universal set of absorption coefficients exists which can be used to determine particle and chlorophyll concentrations in lakes.

Acknowledgments

This research was conducted in cooperation with the U.S. Environmental Protection Agency, University of Wisconsin-Milwaukee Center for Great Lakes Studies, NASA Global Change Fellowship Program, National Research Council Associateship Program, and the North Temperate Lakes-Long Term Ecological Research Program. Reviews by Randolph Wynne, Jonathan Chipman, and Arthur Brooks were appreciated.

Reference Cited

Beeton, A. M., J. W. Moffett, and D. C. Parker. 1969. Comparison of thermal data from airborne and vessel surveys of Lake Erie, *Proc. 12th Conf. Great Lakes Res.* p.513-527.

Bolgrien, D.W. 1993. Delineation of the hydrodynamics of Lake Michigan and Lake Baikal using satellite-derived surface temperatures. Ph.D. Dissertation, University of Wisconsin-Milwaukee.

Bolgrien, D. W., and A. S. Brooks. 1992. Analysis of thermal features of Lake Michigan from AVHRR satellite images, *J. Great Lakes Research* 18:259-266.

Bolgrien, D. W., N. G. Granin, and L. A. Levin. 1995a. Surface temperature dynamics of Lake Baikal observed from AVHRR images, *Photogrammetric Engineering & Remote Sensing*, 61(2):211-216.

Bolgrien, D.W., R..C. Wrigley, R.A. Armstrong, A.S. Brooks. 1995b. Absorption spectra for chlorophyll, particles, and dissolved organic carbon in Green Bay, Lake Michigan, Proceedings of the 3rd Conference on Remote Sensing for Marine and Coastal Environments, Seattle.

Bukata, R.P., J.E. Bruton, and J.H. Jerome. 1985. Application of direct measurements of optical parameters to the estimation of lake water quality indicators. Scientific Series No. 140. Inland Waters Directorate, National Water Research Institute, Canadian Center for Inland Waters, Burlington, Ont.

Bukata, R.P., J.H. Jerome, and J.E. Bruton. 1988. Particulate concentrations in Lake St. Clair as recorded by a shipborne multispectral optical monitoring system, *Remote Sensing of Environment* 25:201-229.

Bukata, R. P., J. H. Jerome, K. Ya. Kondratyev, and D. V. Pozdnyakov. 1991a. Estimation of organic and inorganic matter in inland waters: optical cross sections of lakes Ontario and Ladoga, *J. Great Lakes Research* 17:461-469.

Bukata, R. P., J. H. Jerome, K. Ya. Kondratyev, and D. V. Pozdnyakov. 1991b. Satellite monitoring of optically-active components of inland waters: an essential input to regional climate change impact studies, *J. Great Lakes Research* 17:470-478.

Bukata, R. P., J. H. Jerome, K. Ya. Kondratyev, and D. V. Pozdnyakov. 1995. Optical Properties and Remote Sensing of Inland and Coastal Waters. CRC Press.

Chambers, R. L., and B. J. Eadie. 1981. Nepheloid and suspended particulate matter in southeastern Lake Michigan, *Sedimentology* 28:439-447.

Church, P. E. 1945. The annual temperature cycle of Lake Michigan. II. Spring warming and summer stationary periods, 1942. Misc. Report 18, University of Chicago, Inst. Meteorol.

Gallie, E.A., and P.A. Murtha. 1992. Specific absorption and backscattering spectra for suspended minerals and chlorophyll *a* in Chilko Lake B.C., *Remote Sensing of Environment* 39:103-118.

Garver, S.A., D.A. Siegel, and B.G. Mitchell. 1994. Variability in near-surface particulate absorption spectra: what can a satellite ocean color imager see? *Limnol. Oceanogr.* 39:1349-1367.

Gordon, H. R., J. L. Clark, J. L. Mueller, and W. A. Hovis. 1980. Phytoplankton pigments from the Nimbus-7 Coastal Zone Color Scanner: comparison with surface measurements, *Science* 210:63-66.

Gottlieb, E. S., J. H. Saylor, and G. S. Miller. 1990. Currents and water temperatures observed in Green Bay, Lake Michigan - Part I: winter, 1988-1989; Part II: Summer 1989, NOAA Technical Memorandum ERL GLERL-73. 90 p.

Lane, R. K. 1970. Great Lakes thermal studies using infrared imagery, *Limnol. Oceanogr.* 15(2):296-302.

Lathrop, R. G. 1992. Landsat Thematic Mapper monitoring of turbid inland water quality, *Photogrammetric Engineering & Remote Sensing* 58(4):465-470.

Lathrop, R. G., and T. M. Lillesand. 1986. Use of Thematic Mapper data to assess water quality in Green Bay and Central Lake Michigan, *Photogrammetric Engineering & Remote Sensing* 52(5):671-680.

Lathrop, R. G., and T. M. Lillesand. 1987. Calibration of thematic mapper thermal data for water surface temperature mapping: case study on the Great Lakes, *Remote Sensing of Environment* 22:297-307.

Lathrop, R. G., and T. M. Lillesand. 1989. Monitoring water quality and river plume transport in Green Bay, Lake Michigan with SPOT-1 imagery, *Photogrammetric Engineering & Remote Sensing* 55(3):349-354.

Lathrop, R. C., J. R. Vande Castle, and T.M. Lillesand. 1990. Monitoring river plume transport and mesoscale circulation in Green Bay, Lake Michigan through satellite remote sensing, *J. Great Lakes Research*, 16:471-484.

Leshkevich, G. A., D. J. Schwab, and G. C. Muhr. 1993. Satellite environmental monitoring of the Great Lakes: a review of NOAA's Great Lakes CoastWatch Program, *Photogrammetric Engineering & Remote Sensing* 59(3):371-379.

Lesht, B. M., and D. J. Brandner. 1992. Functional representation of Great Lakes surface temperatures, *J. Great Lakes Research* 18(1):98-107.

Maturi, E. M., and K. G. Taggart. 1993. Great Lakes CoastWatch Users Guide, NOAA National Environmental Satellite, Data, and Information Service, Office of Research and Applications, Satellite Applications Laboratory, Washington, DC.

McFadden, J. D., and R. A. Ragotzkie. 1963. Aerial mapping of surface temperature pattern of Lake Michigan, *Publ. No. 10, Great Lakes Res. Div.*, University of Michigan.

Mitchell, B.G. 1990. Algorithms for determining the absorption coefficient of aquatic particulate using the Quantitative Filter Technique (QFT), *SPIE 1302 Ocean Optics* X:137148.

Mitchell, B.G., and D.A. Kiefer. 1988. Variability in pigment specific fluorescence and absorption spectra in the northeastern Pacific Ocean, *Deep Sea Research* 35:665-689.

Moll, R. A., A. Bratkovich, W. Y. B. Chang, and P. Pu. 1993. Physical, chemical, and biological conditions associated with the early stages of the Lake Michigan vernal thermal front, *Estuaries*, 16(1):92-103.

Morel, A., and L. Prieur. 1977. Analysis of variations in ocean color, *Limnol. Oceanogr.* 22:709-722.

Mortimer, C. H. 1968. Internal waves and associated currents observed in Lake Michigan during the summer of 1963. Report No. 1, University of Wisconsin-Milwaukee, Center for Great Lakes Studies.

Mortimer, C. H. 1971. *Large-scale oscillatory motions and seasonal temperature changes in Lake Michigan and Lake Ontario, Parts I & II.* Special Report #12 of the University of Wisconsin-Milwaukee, Center for Great Lakes Studies, 106 p.

Mortimer, C. H. 1988. Discoveries and testable hypotheses arising from Coastal Zone Scanner imagery of southern Lake Michigan, *Limnol. Oceanogr.*, 33:203-226.

Noble, V. E., and J. C. Wilkerson. 1970. Airborne temperature surveys of Lake Michigan, October 1966 and 1967, *Limnol. Oceanogr.* 15(2):289-296.

Roesler, C.S., M.J. Perry, and K.L. Carder. 1989. Modeling *in situ* phytoplankton absorption from total absorption spectra in productive inland marine waters, *Limnol. Oceanogr.* 34:1510-1523.

Sager, P.E. and S. Richman. 1991. Functional interaction of phytoplankton and zooplankton along the trophic gradient in Green Bay, *Can. J. Fish. Aquat. Sci.* 48:116-122.

Scarpace, F. L., T. Green, and R. P. Madding. 1979. A thermal scanning study of coastal upwelling in Lake Superior, *Proc. Am. Soc. Photogrammetry*, p.349-378.

Schluessel, P., W. J. Emery, H. Grassi, and T. Mammen. 1990. On the bulk-skin temperature difference and its impact on satellite remote sensing of sea surface temperature, *J. Geophysical Res.* 95(C8):13341-13356.

Schwab, D. J., G. A. Leshkevich, and G. C. Muhr. 1992. Satellite Measurements of surface water temperature in the Great Lakes - Great Lakes CoastWatch, *J. Great Lakes Research* 18(2):247-258.

Smith, R.C., and K.S. Baker. 1981. Optical properties of the clearest natural waters (200-800 nm), *Applied Optics* 20:177-184.

Tanis, F. J. 1984. Phase II development of Great Lakes algorithms for Nimbus-7 Coastal zone color scanner, Final Report 157900-23-F Environmental Res. Inst. of Michigan, Ann Arbor MI.

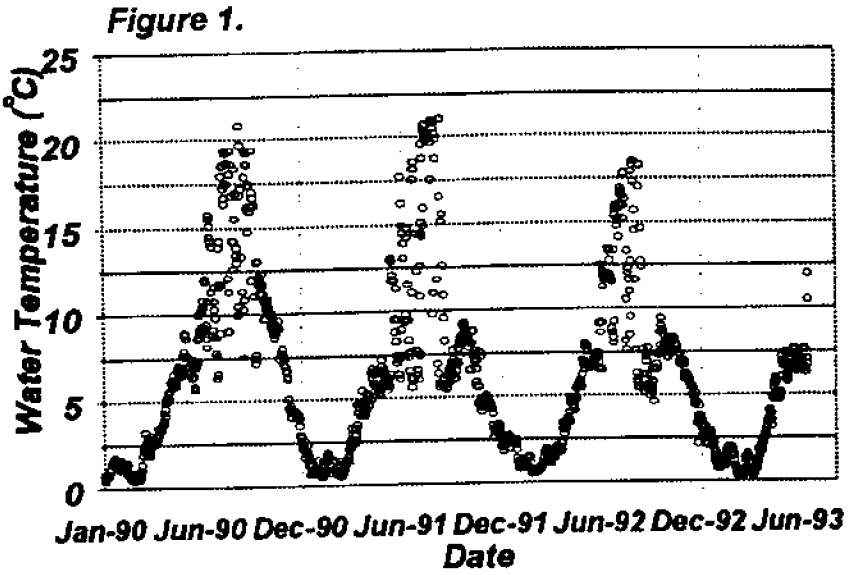

Figure 1. Daily mean temperatures from the Milwaukee, WI. Linnwood Filtration Plant. The water intake crib is located at 43.08°N x 87.84°W in 22 m of water approximately 2 km from shore. Water is drawn from 4 m off the bottom.

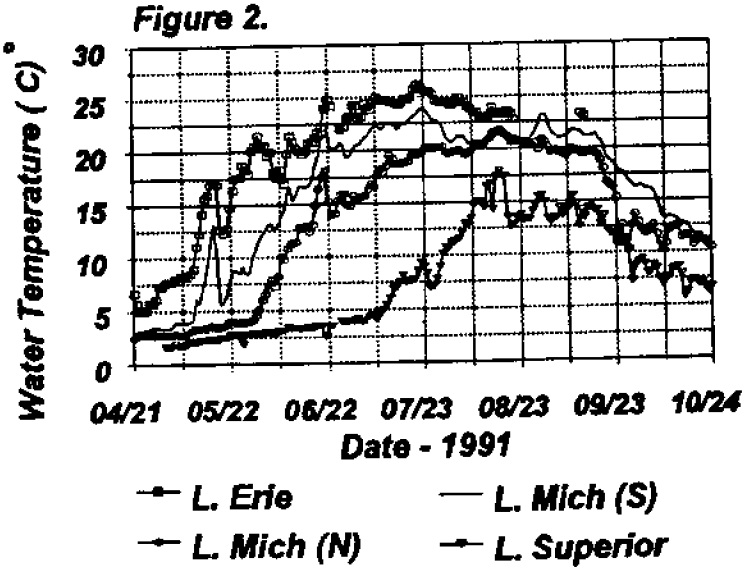

Figure 2. Surface (0.5 m) water temperature (°C) measured at NDBC meteorological buoys in Lake Erie (41.7°N x 82.4°W), southern Lake Michigan (S) (42.7°N x 87.1°W), northern Lake Michgian (45.3°N x 86.4°W), and Lake Superior (48.0°N x 87.7°W). Data collected 12 April - 15 October, 1991.

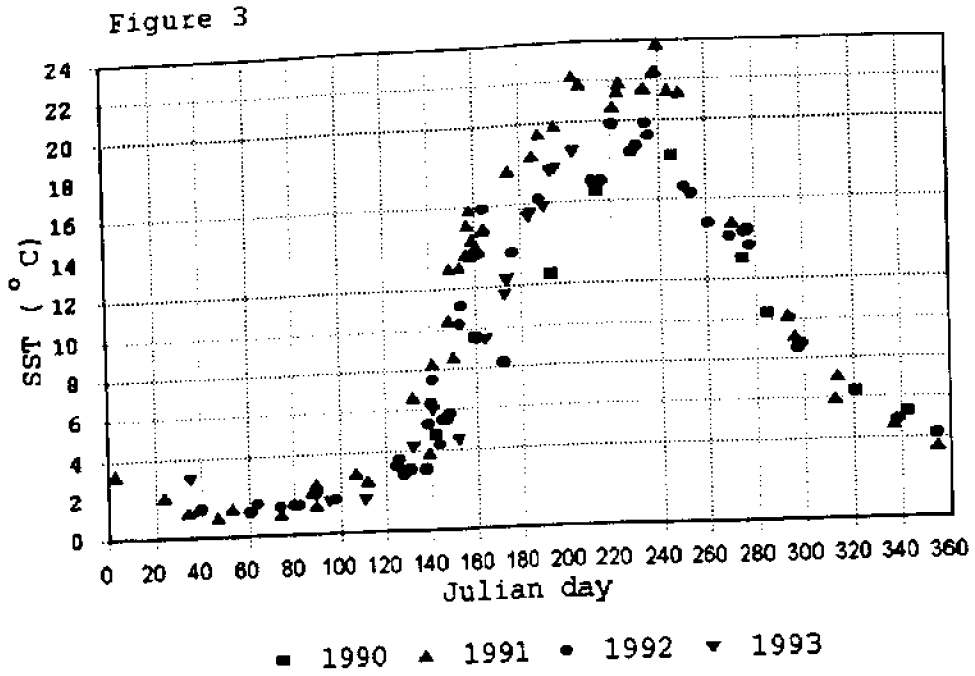

Figure 3. Median AVHRR-derived SST images (<20% cloud cover) of Lake Michigan, 20 May, 1990 - 5 July, 1993. To exclude clouds, ice, and land pixels, SST were restricted to values between 1°C and 27°C.

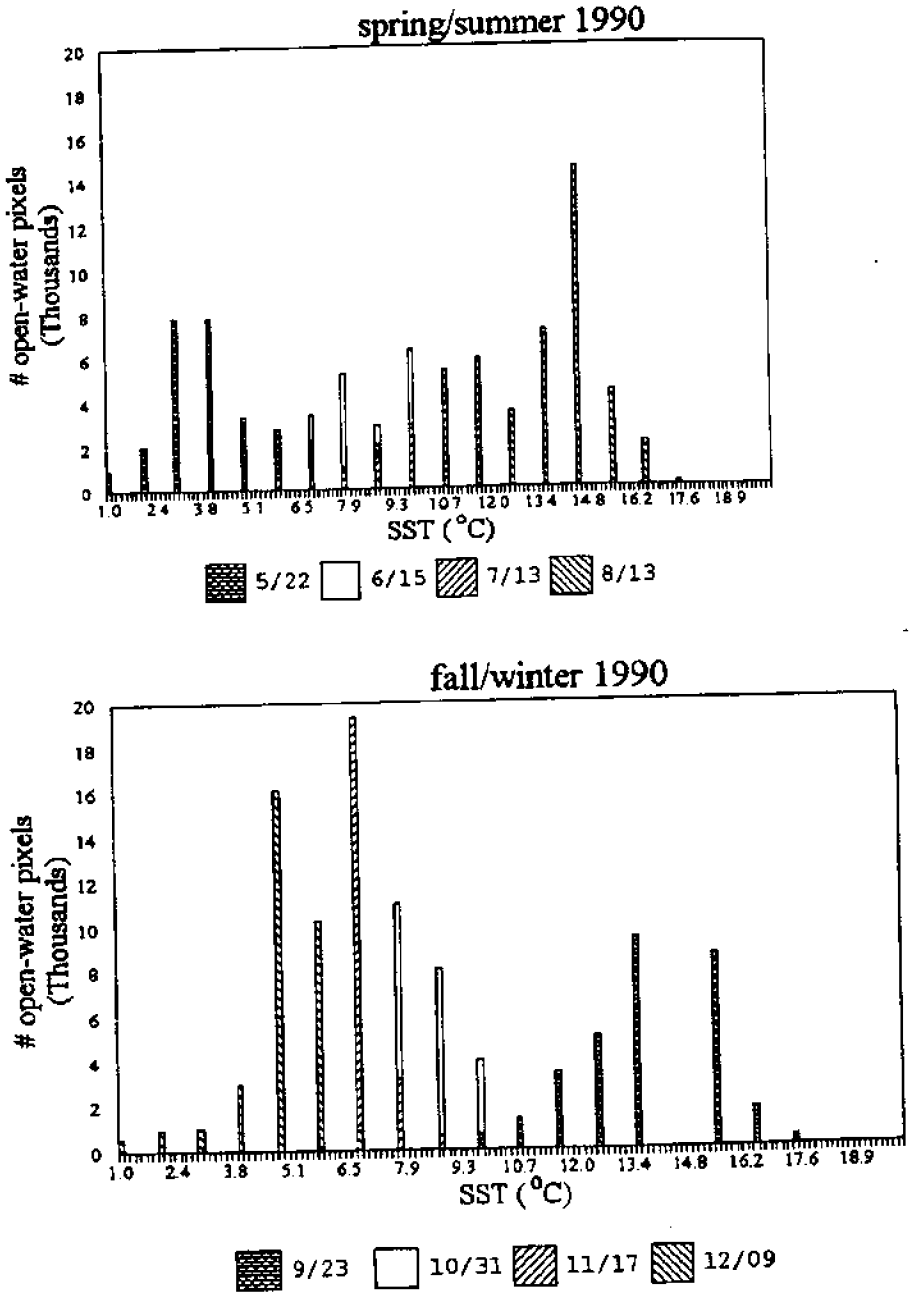

Figure 4. Frequency distribution of SST of Lake Michigan in 1990. SST values were restricted between 1°C and 27°C. Values are % of the 33,700 openwater (cloud-free & ice-free) pixels of the lake. Each pixel is approximately 1.7 km^2 (based on an average 1.3 km pixel width at 44°N): a) spring/summer warming; b) fall cooling

Figure 5

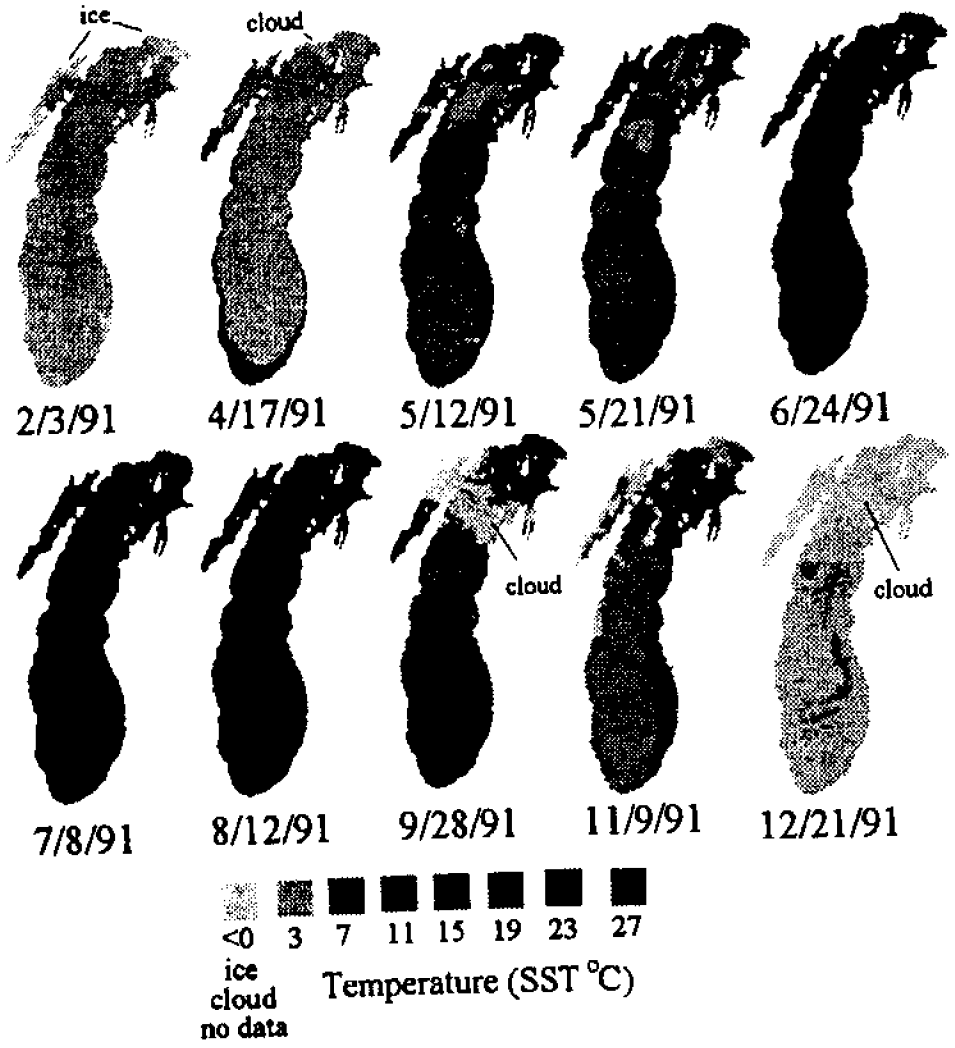

Figure 5. AVHRR SST (°C) images of Lake Michigan depicting the seasonal temperature cycle in 1991.

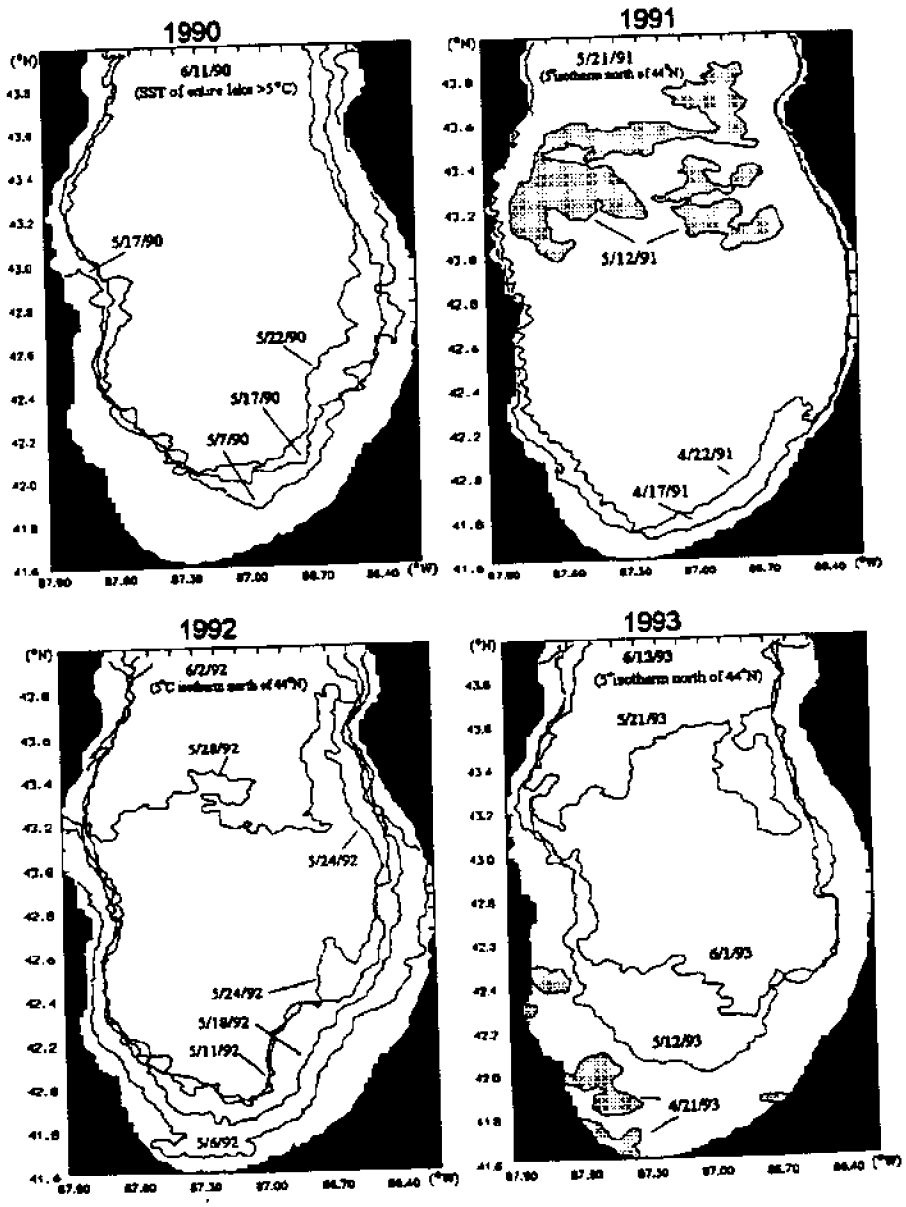

Figure 6. Schematic diagram showing the migration of the vernal thermal front in southern Lake Michigan by plotting the position of the 5°C isotherm. The 5°C isotherm nominally represents the position of the thermal front.

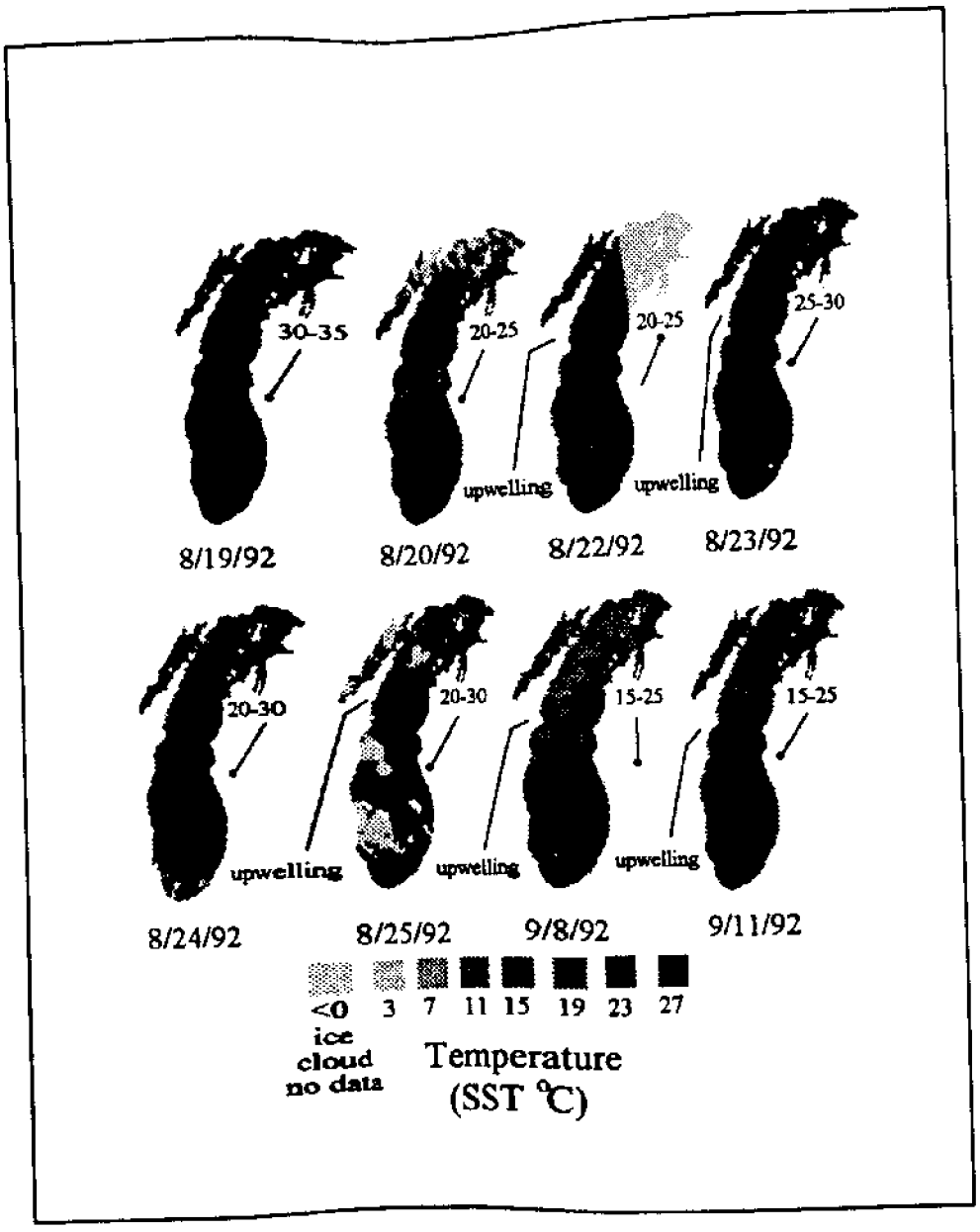

Figure 7. AVHRR SST (° C) images of Lake Michigan depicting upwelling in August-October, 1992. Wind direction and speed ($km \cdot h^{-1}$) recorded at the NDBC buoys are noted. Wind was blowing in the direction the tail is pointing.

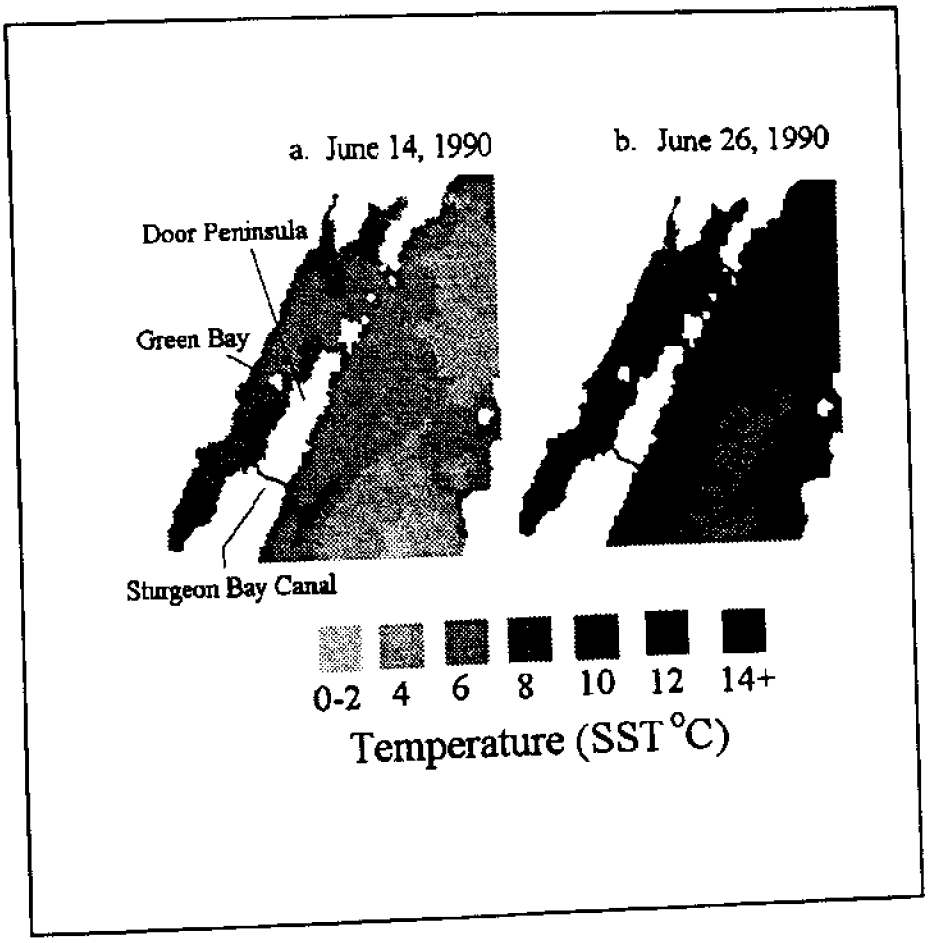

Figure 8. AVHRR SST (°C) images of Green Bay and Lake Michigan showing the intrusion of warmer bay water into the lake: a) 14 June 1990 showing a warm water plume near the Sturgeon Bay canal; b) 26 June 1990 showing a warm water plume near the mouth of Green Bay.

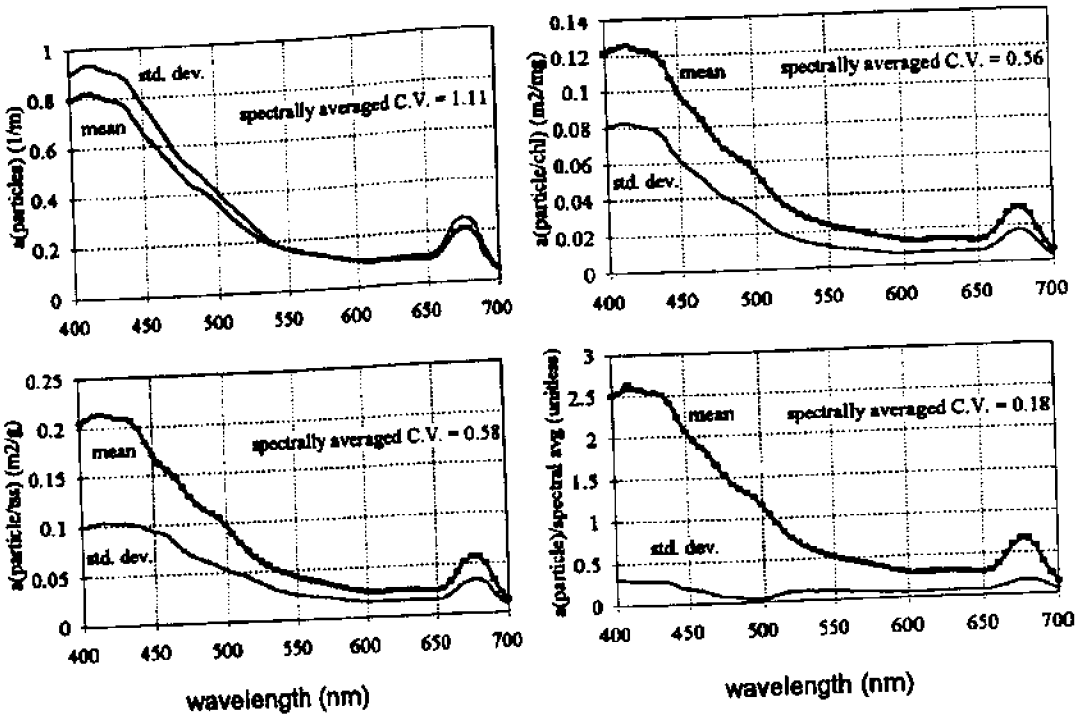

Figure 9. Mean and standard deviation of total particle absorption spectra ($a_{particle}$; m^{-1}) , chlorophyll-specific absorption spectra ($a_{particle}$·[chl]$^{-1}$; $m^2 \cdot mg^{-1}$), TSS-specific absorption spectra ($a_{particle}$·[tss]$^{-1}$; $m^2 \cdot g^{-1}$), and normalized absorption spectra ($a_{particle}(\lambda)$·(mean $a_{particle}$)$^{-1}$; unitless) (see text).

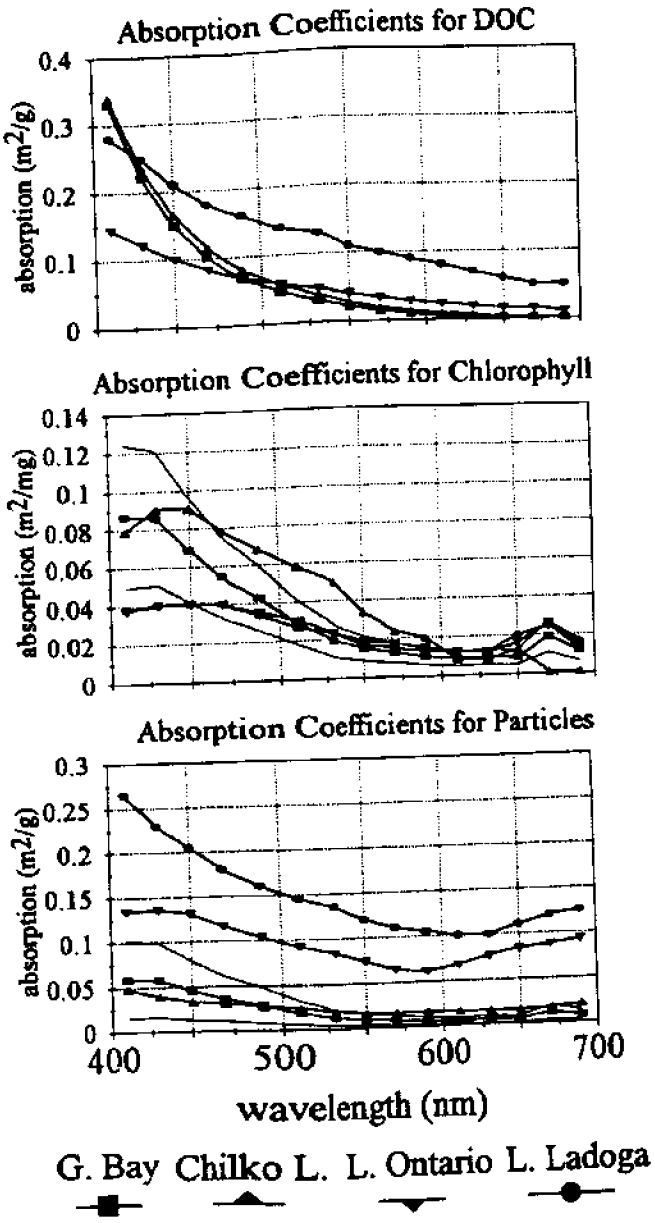

Figure 10. Comparison of absorption coefficients for dissolved organic carbon ($m^2 \cdot g^{-1}$), chlorophyll ($m^2 \cdot mg^{-1}$), and total suspended particles ($m^2 \cdot g^{-1}$) for Green Bay and other lakes (Chilko Lake (Gallie and Murtha 1992); Lake Ontario (Bukata *et al.* 1985); Lake Ladoga (Bukata *et al.* 1991a)).

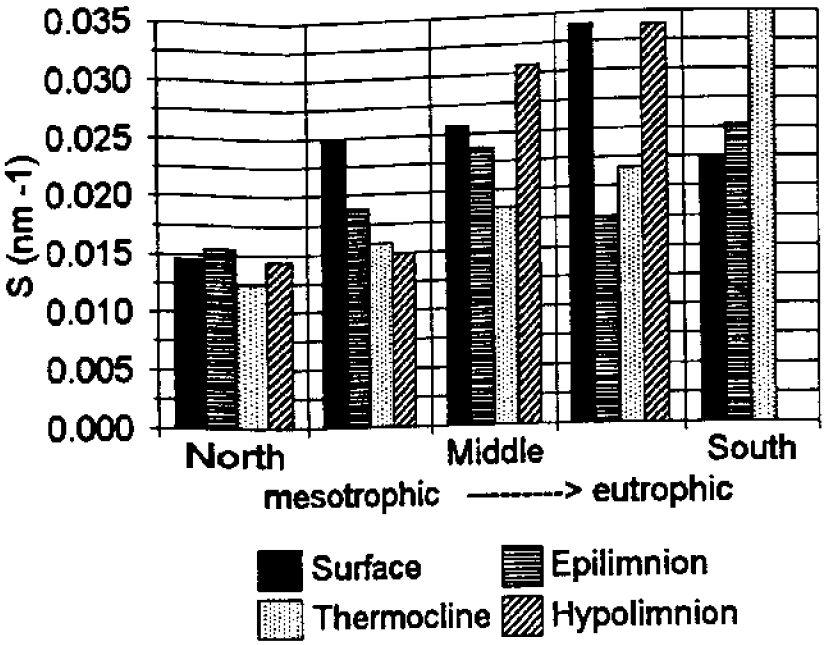

Figure 11. Distribution of spectral light extinction coefficients (S; nm^{-1}) in Green Bay.

List of figures

A NEW WATER QUALITY THREAT IN LAKE MICHIGAN: SUBMERGED VEGETATION - HELP FROM NOAA'S COASTAL-CHANGE ANALYSIS PROGRAM (C-CAP)

Randy Ferguson
Technical Coordinator, NOAA C-CAP
National Marine Fisheries Service, Beaufort, NC Laboratory

Summarized by:
Christine H. Pennisi
Marine Extension Educator, Illinois - Indiana Sea Grant Program

Much of the water in Lake Michigan, along with many parts of the other Great Lakes, is becoming clearer; however, it is not understood whether this is part of normal cycling or due to some atypical cause. In any case, as a result, more macrophytic aquatic plants are now growing in protected areas of the shoreline, where they have not grown before, or at least, for many years. One problem that this is beginning to cause is the interruption of normal littoral and offshore currents. These currents have been relied upon to replenish nearshore areas with constant water change.

Now with the littoral and offshore drift interrupted along some macrophytic beds, nearshore water is slower to replenish. If a wastewater outfall happens to be in that vicinity, wastewater may remain in the area of the outfall instead of dispersing. Since many nearshore areas are used for recreation and drinking water, a health hazard is emerging in areas where nearshore water containing wastewater is trapped near the shoreline close to areas of human contact.

The NOAA C-CAP program could be helpful in determining where and to what extent these submerged aquatic plant beds occur off the southern Lake Michigan shoreline. This information, in turn, could help define whether and to what extent this potential health threat might be in these waters. The NOAA C-CAP program is synopsized below.

What is the Coastal Change Analysis Program?

The Coastal Change Analysis Program (C-CAP) is a partnership among NOAA's National Marine Fisheries Service, National Ocean Service, and Coastal Services Center (CSC). C-CAP classifies types of land cover, analyzes and monitors changes in coastal

submersed habitats, wetlands habitats, and adjacent uplands using remote-sensing techniques (satellite imagery and aerial photography). Through this analysis, scientists hope to correlate the changes in terrestrial regions with those in coastal aquatic habitats, and with changes in the distribution, abundance, and health of living marine resources.

Remote sensing is the gathering of information about an object from some distance. Your eyes are examples of remote-sensing devices. Remote-sensing instruments aboard aircraft or satellites detect various types of electromagnetic energy emitted or reflected from the Earth's surface. This bird's-eye view allows C-CAP to analyze and compare information over large areas of the Earth.

How does CSC support the coastal resource management community through C-CAP?

Some of the areas in which land cover change information can support resource management include: planning of land resources, detecting nonpoint-source pollution, ensuring compliance with zoning laws, and predicting the impact of land cover changes on fisheries.

One region in which CSC scientists are presently working with resource managers is the Columbia River Estuarine area of Washington and Oregon. This area includes Willapa Bay, one of the most productive shellfish fisheries in the country. C-CAP, working with local resource experts, is using satellite imagery to verify and update land cover information, such as wetlands, forested areas, and developed or barren regions, and to assess the changes in land cover over time. Area resource managers are particularly interested in this analysis, since the information is helpful in predicting the impact of land cover change on the region's shellfish beds and salmon fisheries. Data retrieved from these land cover analyses have been used to help local planning commissions determine compliance with zoning laws.

Land cover and change maps can be integrated with other spatially referenced data in a geographic information system (GIS), which can provide resource managers with additional tools and information. For example, C-CAP supported Maine salmon fisheries managers by providing satellite-derived land cover change information, which was then integrated with data on stream networks and salmon nesting habitats in a GIS. Area coastal managers used this integrated information to make predictions concerning the impact of forestry practices on salmon nesting areas.

What services can CSC provide through the Coastal Change Analysis Program?

C-CAP can provide direct assistance to local, state, and regional coastal resource managers in developing new C-CAP products. C-CAP usually works with cooperators in one of two ways:

- C-CAP can perform the change-detection analysis in-house, working with local cooperators to collect ground data and assess the accuracy of the change analysis.

- For cooperators with image-processing expertise, C-CAP can provide imagery, technical assistance, and instruct operators in C-CAP processing techniques to ensure that all products generated will meet the standards of and are consistent with the C-CAP national database

Specific products that are presently available include CD-ROM's of land cover change in:

Chesapeake Bay	1984 and 1988/89
Maine	1985 and 1992
Alaska	1986 and 1993
Columbia River Area (WA/OR)	1989 and 1992

CD-ROM coverages nearing completion include: San Francisco Bay, South Carolina, North Carolina, South Florida, and Texas. In the future, land cover change data will be available for all coastal areas of the U.S., including Alaska, Hawaii, and the Great Lakes.

How can C-CAP help the Southern Lake Michigan Region?

As noted above, C-CAP does include the Great Lakes coastal areas. With assistance of C-CAP, both Illinois and Indiana Department of Natural Resource agencies could obtain current remote sensing imagery of the offshore aquatic plant beds. These could be compared to possible wastewater outfalls or tributaries and to areas of recreational or drinking water intake pipes to determine areas of potential health threat. This critical information can be used in several shoreline-oriented policy decisions ranging from scaling back outfall amounts during periods of great aquatic weed growth to the closing of some recreational beaches during the same time.

How can I obtain more information regarding the Coastal Change Analysis Program?

For more information on CSC's Coastal Change Analysis Program, contact Don Field, (803) 974-6233; dfield@csc.noaa.gov

WHAT REMOTE SENSING CAN ADD TO WATER QUALITY DECISION-MAKING

Fred Tanis
Center for Earth Sciences
Environmental Research Institute of Michigan (ERIM)

Summarized by:
Christine H. Pennisi
Marine Extension Educator, Illinois - Indiana Sea Grant Program

Optical and microwave remote sensing data has long been used in the analysis of coastal and ocean environments; this can include that of water quality analysis in the Great Lakes region. A synopsis of how and why this is done follows.

Overview and Perspectives

- Access to value added remote sensing data products is enhanced by the technology developments in the "age of information";
- Decision makers need experts to provide high quality condensed information;
- Users need to actively participate in the specification of remote sensing data requirements;
- Prospects for participation by federal agencies and commercial interests will depend on an active data user community;
- There appears now to be a long-term commitment to provide extensive earth remote sensing data;
- In the future, costs for data conditioning will likely be transferred to the user community, and the user must become an active team member in product development, and;
- Once remote sensing data are conditioned, they can be easily integrated with other environmental data for purposes of monitoring, assessment and decision making.

A Recommended Pilot Study for the Water Quality Interests

An innovative concept is recommended for pilot-testing to facilitate linking more effectively and efficiently the Great Lakes water quality management community with the remote sensing community. The following points were outlined:

Assumption: There exists sufficient regional remote sensing expertise, data processing facilities, and data distribution networks to support the development of a regional cooperative facility.

Approach:

- Plan a distributed cooperative facility for Great Lakes satellite information;
- Set goals for product development and select satellite and environmental data resources;
- Transfer a common set of tools and database structures of the Strategic Environmental Research and Development Program to each participant;
- Link the distributed user community with the GLIS and GLEIS information networks;
- Target several streams of satellite data for the information cooperative demonstration;
- Participate as a team for satellite product development. Products are distributed and added as part of the database at each node. The original satellite data remains a distributed resource, and;
- Evaluate the utility of data products developed by the cooperative.

Expected Result:

- Recommendations for satellite data integration and product development in support of water quality management, and;
- Demonstration products supporting basic and applied research interests.

A flow-chart further illustrating this concept is illustrated in Figure 1.

A similar concept applied to the San Diego Bay region. Because this Bay has intense competition of use between the military, commercial and recreational interests, it mimics in a smaller way similar water quality concerns in the Great Lakes region. A similar flowchart as the one provided and titled, the Strategic Environmental Research and Development Program was comprehensively developed for San Diego Bay and was the prototype for this one.

A similar comprehensive information system could be developed around Figure 1 based on the expertise developed from the San Diego Bay study and its implementation. Sea Grant was recommended to lead this effort.

GREAT LAKES SATELLITE INFORMATION SYSTEM

A Cooperative Virtual Facility Concept

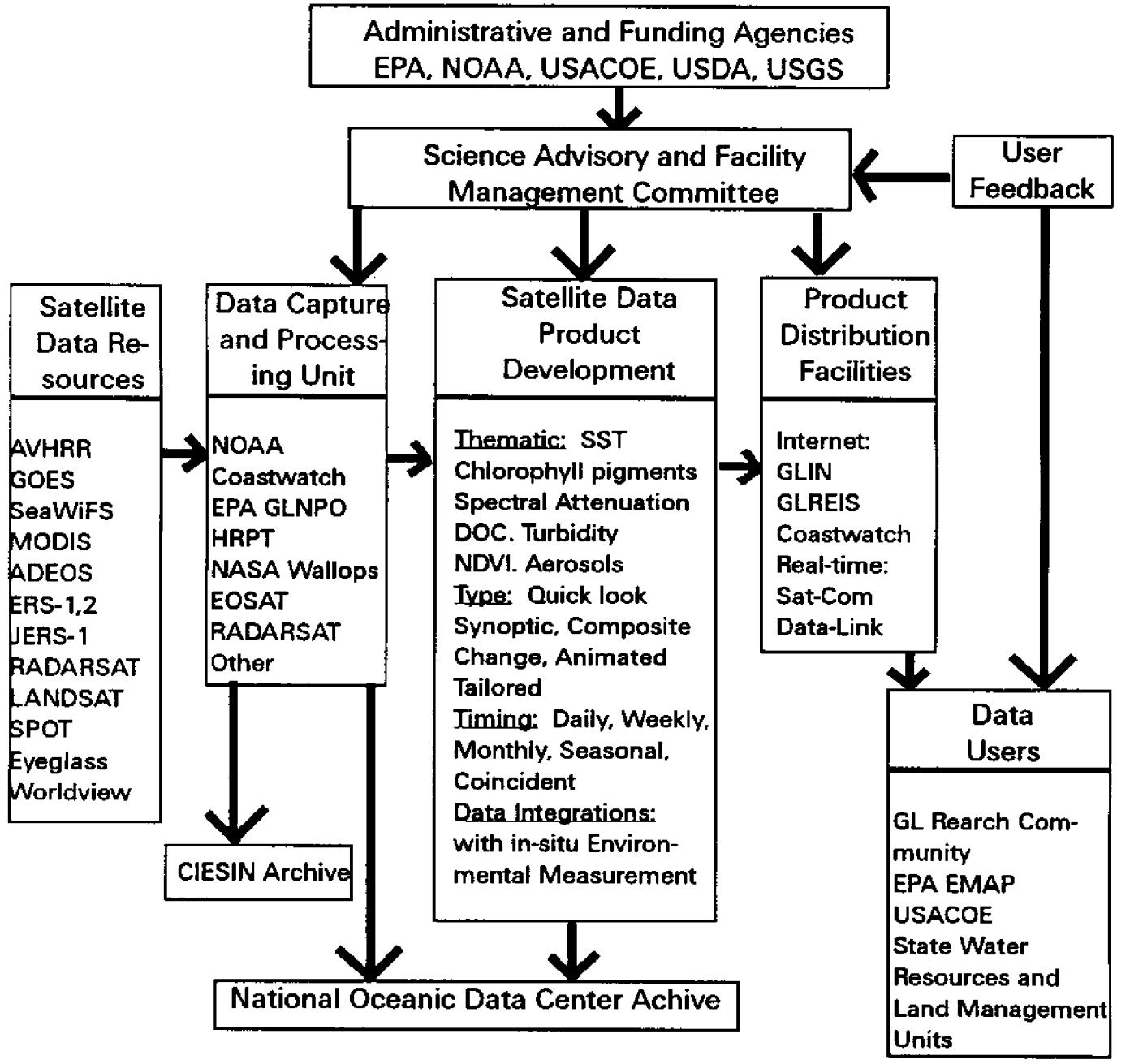

Figure 1